JOURNAL OF OPTOELECTRONICS AND ADVANCED MATERIALS, Vol. 11, No. 4, April 2009, p. 369 - 379

Band ferromagnetism in systems of variable dimensionality II: the two-dimensional finite-temperature case

G. A. LUNGU*, C. M. TEODORESCU
National Institute of Materials Physics, P.O. box MG-7, Bucharest-Magurele, Ilfov, 077125, Romania

In a previous paper [C.M. Teodorescu and G.A. Lungu, J. Optoelectron. Adv, Mater. **10**, 3058 (2008)] we studied the zero temperature problem of the occurence of band ferromagnetism and of the derivation of the Stoner criterion for systems of variable dimensionality: 1D, 2D, 3D. The dimensionality of the system is reflected by a different shape of the density of states. For ideal 2D systems, the density of states is a constant and this seems to be the simplest case to be modelled. In this paper we integrate to this simplest model of constant density of states the influence of temperature, in order to analyse temperature-dependent ferromagnetism in two-dimensional systems, such as magnetic surfaces. Some surprising results are obtained, namely: (i) in contrast to the common belief, in this case the influence of the temperature is to favour, not to inhibit ferromagnetism, i.e. in some conditions ferromagnetism may be obtained at finite temperature, even for systems where the zero temperature Stoner criterion is not satisfied; (ii) for a careful choice of the ratio between the Hubbard energy parameter U and the equilibrium zero-temperature Fermi level value $\varepsilon_F(0)$, systems nonmagnetic at low temperature which become magnetic at higher temperature may be possible. A short review of the experimental data which may be interpreted within the present formalism is also given.

(Received March 25, 2009; after revision April 24, 2009; accepted April 25, 2009)

Keywords: Low-dimensional systems, Ferromagnetism, Stoner criterion, Surfaces

1. Introduction

Since the original paper of Stoner [1], many studies treated the band ferromagnetism, since it is a resonable alternate model to magnetism of localized moments for explaining magnetism in metals. Nowadays, these studies are revigorated, especially dealing with magnetism in low-dimensional systems of delocalized electrons, mainly because of recent achievements in the experimental synthesis of such systems [2,3]. We note the quite recent report on the experimental evidence of ferromagnetic order in nickel single atomic layers on Cu(001) [4], and of linear decrease of magnetisation with temperature, which was treated in a model of 2D spin waves.

Recent studies of surface magnetism revealed exciting trends, mainly the possibility of synthesis of ferromagnetic surfaces from materials which are not ferromagnetic in the bulk. In 2000, the synthesis of magnetic *hcp* chromium grown on Ru(0001) was reported [5]. In 2001, the long-standing problem of the magnetism of the c(2×2) Mn grown on Cu(001) was shown to exhibit ferromagnetism [6], and in 2003 magnetic vanadium was synthesized on Cu(001) in the form of small aggregates grown at very low temperature [7]. The generic affirmation that "the Stoner criterion is satisfied in surfaces, whereas it is not satisfied in the bulk material" is somehow misleading, in the absence of a detailed knowledge of the density of states of the above mentioned surfaces. In this work, we intend to systematically investigate the occurence of ferromagnetism as function on temperature in metal surfaces and to compare the theoretical findings with recent available experimental data.

In a previous paper [8], we treated the zero temperature case for the occurence of band ferromagnetism in systems of variable dimensionality. The dimensionality of the system is taken into accont *via* the energy dependence of the equilibrium density of states $g(\varepsilon) \sim \varepsilon^{1/2}$ for 3D, $g(\varepsilon) \sim \text{const.}$ for 2D, and $g(\varepsilon) \sim \varepsilon^{-1/2}$ for 1D. The ferromagnetic interaction occurs *via* the Hubbard energy term $-U\xi^2/4$, where ξ is the polarization fraction: $n\xi/2$ electrons per unit volume passed from the minority spin sub-band to the majority spin sub-band (where n is the total electron density). Therefore, the Fermi levels will be different for the majority and for the minority sub-bands $\varepsilon_F^{\uparrow}$ and $\varepsilon_F^{\downarrow}$, functions on ξ. This allows to compute the kinetic energy increase due to the spin polarization and then the total energy variation $\Delta w(\xi)$. Stable states are obtained when $\Delta w(\xi)$ exhibits a minimum. The Stoner criterion examines the stability of the paramagnetic state $\xi = 0$; indeed, it may be shown that the energy always exhibits an extremum at $\xi = 0$, but, in order to obtain ferromagnetism, this extremum must be a maximum, i.e. $\partial^2(\Delta w)/\partial\xi^2$ must be negative. This inequality is readily transformed in a condition between the relevant parameters of the model (e.g. Hubbard energy, equilibrium Fermi level), which is called the Stoner criterion [1].

In the present study, we aim to integrate the temperature in the simplest model, that is, constant density of states, representing two-dimensional systems. The same procedure as in [8] will be followed: in Sec. 2 we describe the relevant parameters of the polarized sub-bands, in Sec. 3 we compute the total energy, then in Sec. 4 its first derivative. Before computing the second derivative, we must stop on some novel aspects evidenced by these 2D systems, i.e. on the co-existence of ferromagnetism and paramagnetism in a certain region of the parameter space. Both states correspond to local minima. One state (ferromagnetic or paramagnetic) is represented by the absolute minimum, being then the most stable state, while the other state of the system is metastable, corresponding to a relative minimum (Sec. 5). In Sec. 6 we investigate the possibility of engineering novel systems starting with the present study, i.e. systems which are paramagnetic at low temperature and become ferromagnetic by *rising* the temperature. In Sec. 7 we will compute the second-order derivative of the energy and derive a temperature-dependent Stoner criterion, while Sec. 8 presents some conclusions.

A problem which will be just outlined in this work is the behaviour of the system near the critical point (Curie temperature). This is a separate work and will be detailed in another paper. Nevertheless, an outline about the behaviour near the critical point will be sketched in the Conclusions paragraph.

In the following, we will continue with some notations of the problem.

For the finite temperature case of two-dimesional free electron model, the density of states is supposed to be constant, that is

$$g_0 = g_\uparrow = g_\downarrow = \frac{n}{2\varepsilon_F(0)} \tag{1}$$

where $\varepsilon_F(0)$ is the zero temperature Fermi level.

Thus, the number of electrons in equilibrium state for a sub-band $\uparrow$ or $\downarrow$ is

$$\begin{aligned} n_0 = \frac{n}{2} &= \int_0^\infty g_0 f(\varepsilon, T) d\varepsilon \\ &= \frac{n}{2\varepsilon_F(0)} \int_0^\infty \frac{d\varepsilon}{\exp\left[\frac{\varepsilon - \varepsilon_F(T)}{k_B T}\right] + 1} \end{aligned} \tag{2}$$

with $\varepsilon_F(T)$ being the finite temperature Fermi level, and $f(\varepsilon, T)$ the Fermi-Dirac distribution function.

With the same notations $\varepsilon_F(0)/k_B T \equiv y_0$ and $\varepsilon_F(T)/k_B T \equiv y$, we may write that

$$n_0 = \frac{n}{2} = \frac{n}{2y_0} \ln(1 + e^y), \tag{3}$$

so we can express the finite temperature Fermi level as function of zero temperature Fermi Level:

$$\varepsilon_F(T) = k_B T \ln\left[\exp\frac{\varepsilon_F(0)}{k_B T} - 1\right] \tag{4}$$

which may also be written for y as function of y_0:

$$y = \ln(e^{y_0} - 1) \tag{5}$$

2. Polarized sub-bands

The electron densities of the spin „up" and spin „down" sub-bands, $n_\uparrow$ and $n_\downarrow$, are obtained as functions of the corresponding temperature-dependent Fermi levels $\varepsilon_F^\uparrow(T)$ and $\varepsilon_F^\downarrow(T)$:

$$n_\uparrow = \frac{n}{2}(1 + \xi) = \frac{n}{2\varepsilon_F(0)} \int_0^\infty \frac{d\varepsilon}{\exp\left[\frac{\varepsilon - \varepsilon_F^\uparrow(T)}{k_B T}\right] + 1} \tag{6}$$

$$n_\downarrow = \frac{n}{2}(1 - \xi) = \frac{n}{2\varepsilon_F(0)} \int_0^\infty \frac{d\varepsilon}{\exp\left[\frac{\varepsilon - \varepsilon_F^\downarrow(T)}{k_B T}\right] + 1} \tag{7}$$

Noting $\frac{\varepsilon_F^\uparrow(T)}{k_B T} \equiv y_\uparrow$ and $\frac{\varepsilon_F^\downarrow(T)}{k_B T} \equiv y_\downarrow$ we obtain expressions similar to Eq. (3):

$$n_{\uparrow\downarrow} = \frac{n}{2}(1 \pm \xi) = \frac{n}{2y_0} \ln(1 + e^{y_{\uparrow\downarrow}}) \tag{8}$$

Conversely,

$$y_{\uparrow\downarrow} = \ln\{\exp[y_0(1 \pm \xi)] - 1\} \tag{9}$$

In the finite temperature case, there exists a maximum value of the polarization, $\xi_{\max}$, corresponding to the displacement of the Fermi level corresponding to the minority sub-band at the minimum available energy, which has been chosen as zero. Setting $y_{\downarrow_{\min}} = 0$, one obtains:

$$\frac{n}{2}(1 - \xi_{\max}) = \frac{n}{2}\ln 2 \Rightarrow \xi_{\max} = 1 - \frac{\ln 2}{y_0} \tag{10}$$

It follows that, if $y_0 \leqslant \ln 2$, no polarization can be achieved, independently of how important the Hubbard interaction parameter U is. The maximum position of the Fermi level for the majority spin sub-band is

$$y_{\uparrow_{\max}} = \ln\left(\frac{1}{2}e^{2y_0} - 1\right). \tag{11}$$

Note also that in this case the shift towards higher energies of the majority spin Fermi level is not equal to the shift towards lower energies of the minority spin Fermi level:

$$y_{\uparrow_{\max}} - y = \ln \frac{e^{2y_0} - 2}{2(e^{y_0} - 1)} \neq y - y_{\downarrow_{\min}} = y = \ln(e^{y_0} - 1) \tag{12}$$

(unless $y_0 = \ln 2$).

The above statement is valid for any value of the non-zero polarization:

$$y_{\uparrow} - y = \ln \frac{e^{y_0(1+\xi)} - 1}{e^{y_0} - 1} \neq y - y_{\downarrow} = \ln \frac{e^{y_0} - 1}{e^{y_0(1-\xi)} - 1} \tag{13}$$

Using algebra, one can express the magnetic polarization ξ as:

$$\xi = \frac{1}{2y_0} \ln \frac{1 + e^{y_\uparrow}}{1 + e^{y_\downarrow}} \tag{14}$$

3. Total energy

The energy Δw per electron and unit volume may be written as [8]:

$$\Delta w = \frac{1}{\Omega N}(\Delta E_c + \Delta V) = \frac{1}{\Omega N}(E_c - E_c^{(0)} + \Delta V) \tag{15}$$

Where

$$\frac{1}{\Omega N} E_c = \frac{n}{2\varepsilon_F(0)} \int_0^\infty \frac{\varepsilon \, d\varepsilon}{\exp\left[\frac{\varepsilon - \varepsilon_F^\uparrow(T)}{k_B T}\right] + 1} + \frac{n}{2\varepsilon_F(0)} \int_0^\infty \frac{\varepsilon \, d\varepsilon}{\exp\left[\frac{\varepsilon - \varepsilon_F^\downarrow(T)}{k_B T}\right] + 1} \tag{16}$$

With two succesive variable changes $x = \varepsilon/(k_B T)$, and $t = e^{x - y_\uparrow}$ or $u = e^{x - y_\downarrow}$ respectively, one obtains for $(1/\Omega N) E_c$ the following expression:

$$\begin{aligned} \frac{1}{\Omega N} E_c &= \frac{nk_B T}{2y_0} \left[y_\uparrow \ln(1 + e^{y_\uparrow}) + y_\downarrow \ln(1 + e^{y_\downarrow}) \right] \\ &+ \frac{nk_B T}{2y_0} \left\{ \left[\frac{1}{2} \ln t \ln \frac{t}{(t+1)^2} - Li_2(-t) \right] \Big|_{e^{-y_\uparrow}}^{\infty} \right. \\ &\left. + \left[\frac{1}{2} \ln u \ln \frac{u}{(u+1)^2} - Li_2(-u) \right] \Big|_{e^{-y_\downarrow}}^{\infty} \right\} \\ &= \frac{nk_B T}{2y_0} \left\{ \frac{\pi^2}{6} + \frac{1}{2}\left[y_\uparrow^2 + y_\downarrow^2 \right] + Li_2(-e^{-y_\uparrow}) \right. \\ &\left. + Li_2(-e^{-y_\downarrow}) \right\} \end{aligned} \tag{17}$$

where

$$Li_2(x) = \sum_{k=1}^{\infty} \frac{x^k}{k^2} = -\int_0^x \frac{\ln(t-1)}{t} dt \tag{18}$$

is the dilogarithm function defined in the complex plane over the open unit disk [9], and

$$\lim_{a \to \infty} \left[\frac{1}{2} \ln a \ln \frac{a}{(a+1)^2} - Li_2(-a) \right] = \frac{\pi^2}{12}$$

(the limit equals the definite integral $\int_0^\infty \frac{x \, dx}{e^x + 1}$ [10]).

In the same manner, with succesive variable changes $x = \varepsilon/(k_B T)$ and $v = e^{x-y}$, we obtain for $(1/\Omega N) E_c^{(0)}$:

$$\begin{aligned} \frac{1}{\Omega N} E_c^{(0)} &= \frac{nk_B T}{2y_0} [2y \ln(1 + e^y)] + 2 \frac{nk_B T}{2y_0} \times \\ &\times \left[\frac{1}{2} \ln v \ln \frac{v}{(v+1)^2} - Li_2(-v) \right] \Big|_{e^{-y}}^{\infty} \\ &= 2 \frac{nk_B T}{2y_0} \left[\frac{\pi^2}{12} + \frac{1}{2} y^2 + Li_2(-e^{-y}) \right] \end{aligned} \tag{19}$$

thus:

$$\begin{aligned} \frac{1}{\Omega N} \Delta E_c = \frac{nk_B T}{2y_0} \left\{ \frac{1}{2} \left[y_\uparrow^2 + y_\downarrow^2 - 2y^2 \right] \right. \\ \left. + \left[Li_2(-e^{-y_\uparrow}) + Li_2(-e^{-y_\downarrow}) - 2Li_2(-e^{-y}) \right] \right\} \end{aligned} \tag{20}$$

We will be able to express the energy Δw (Eq. (15)) as function of y, $y_\uparrow$ and $y_\downarrow$, knowing that $\Delta V = -nU\xi^2/4$ [1]:

$$\begin{aligned} \Delta w = \frac{nk_B T}{2y_0} \left\{ \frac{1}{2} \left[y_\uparrow^2 + y_\downarrow^2 - 2y^2 \right] + \left[Li_2(-e^{-y_\uparrow}) \right. \right. \\ \left. \left. + Li_2(-e^{-y_\downarrow}) - 2Li_2(-e^{-y}) \right] \right\} - \frac{nU}{4} \xi^2 \end{aligned} \tag{21}$$

with y and $y_{\uparrow\downarrow}$ as functions on y_0 and ξ, given by eqs. (5) and (9), respectively.

By dividing by $nk_B T$ and replacing y, $y_\uparrow$ and $y_\downarrow$ from (5) and (9), one obtains the reduced energy dependence on $u \equiv U/k_B T$, y_0, and ξ:

$$\begin{aligned} \omega(u, y_0, \xi) = \frac{1}{2y_0} \left\{ \frac{1}{2} \ln^2 \left[e^{y_0(1+\xi)} - 1 \right] \right. \\ + \frac{1}{2} \ln^2 \left[e^{y_0(1-\xi)} - 1 \right] - \ln^2(e^{y_0} - 1) \\ + Li_2\left(-\frac{1}{e^{y_0(1+\xi)} - 1} \right) + Li_2\left(-\frac{1}{e^{y_0(1-\xi)} - 1} \right) \\ \left. - 2Li_2\left(-\frac{1}{e^{y_0} - 1} \right) \right\} - \frac{u\xi^2}{4} \end{aligned} \tag{22}$$

Two-dimensional plots of $\omega(u, y_0, \xi)$, by taking u as parameter ($u = 2,\ 5,\ 10,\ 20$), are given in Fig. 1.

One may observe the following: (i) for low values of the equilibrium Fermi energy y_0 (in $k_B T$ units), one obtains a result quite similar to the $T = 0$ case, namely the system has its minimal energy in the state with maximum polarization $\xi = 1$ or $\xi = \xi_{max}$, given by Eq. (10), according to Sec. 2; (ii) increase of the Hubbard energy (also measured in $k_B T$ units) makes this minimum more and more pronounced; (iii) for larger values of y_0, the minimum energy is obtained for the paramagnetic state $\xi = 0$; (iv) however, the general trend of the energy surfaces is quite similar to the $T = 0$ case, represented by the equation

$$\Delta w = \frac{n}{2}\left(\varepsilon_F - \frac{U}{2}\right)\xi^2 \Rightarrow \frac{1}{nk_B T}\Delta w = \frac{1}{2}\left(y_0 - \frac{u}{2}\right)\xi^2 \quad (23)$$

where we divided by a non-vanishing, though small, thermal energy ($k_B T$) and by the total electron density n.

However, there are more subtle differences between the zero- and the finite-temperature cases, which will be outlined below.

4. First derivative of the total energy.

$\partial(\Delta w)/\partial\xi$ is computed by taking into account that the derivative of the dilogarithm is expressed as follows [9]:

$$\frac{\mathrm{d}Li_2(x)}{\mathrm{d}x} = -\frac{1}{x}\ln(1-x) \quad (24)$$

therefore:

$$\frac{\partial(\Delta w)}{\partial\xi} = \frac{nk_B T}{2y_0}\left\{\left[y_\uparrow + \frac{dLi_2(-e^{-y_\uparrow})}{d(-e^{-y_\uparrow})}\frac{d(-e^{-y_\uparrow})}{dy_\uparrow}\right]\frac{\partial y_\uparrow}{\partial\xi} + \left[y_\downarrow + \frac{dLi_2(-e^{-y_\downarrow})}{d(-e^{-y_\downarrow})}\frac{d(-e^{-y_\downarrow})}{dy_\downarrow}\right]\frac{\partial y_\downarrow}{\partial\xi}\right\} - \frac{nU}{2}\xi \quad (25)$$

which has the final expression:

$$\frac{1}{nk_B T}\frac{\partial(\Delta w)}{\partial\xi} = \frac{\partial\omega}{\partial\xi} = \frac{y_0}{2}\left\{\frac{1+\xi}{1-e^{-(1+\xi)y_0}} - \frac{1-\xi}{1-e^{-(1-\xi)y_0}}\right\} - \frac{u\xi}{2} \quad (26)$$

The condition for extremum $\partial(\Delta w)/\partial\xi = 0$ requires either $\xi = 0$, or, for $\xi \neq 0$,

$$\frac{U}{\varepsilon_F(0)} \equiv \frac{u}{y_0} = \frac{\xi^{-1}+1}{1-e^{-(1+\xi)y_0}} - \frac{\xi^{-1}-1}{1-e^{-(1-\xi)y_0}} \equiv a(y_0, \xi) \quad (27)$$

with:

$$\lim_{y_0 \to 0} a(y_0, \xi) = 1 \quad (28)$$

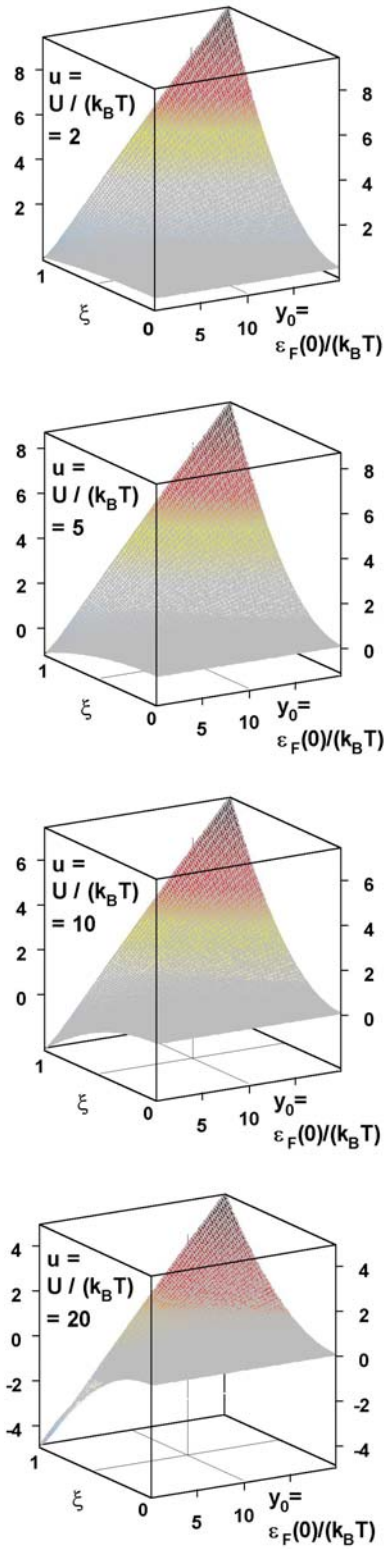

Fig. 1. Plots of the energy $\omega = \Delta w/(nk_B T)$ as function on the asymmetry parameter ξ and on the absolute position of the Fermi level $\varepsilon_F(0)$ in $k_B T$ units $[y_0 = \varepsilon_F(0)/(k_B T)]$, for several values of the Hubbard energy U, also in $k_B T$ units $[u = U/(k_B T)]$.

$$\lim_{y_0\to\infty} a(y_0,\xi) = 2 \tag{29}$$

$$\lim_{\xi\to 0} a(y_0,\xi) = 2\frac{1-(1+y_0)e^{-y_0}}{(1-e^{-y_0})^2} \tag{30}$$

$$\lim_{\xi\to 1} a(y_0,\xi) = \frac{2}{1-e^{-2y_0}} - \frac{1}{y_0} \tag{31}$$

Eq. (31) implies that at low temperatures or high $\varepsilon_F(0)$ ($T\to 0$ or $\varepsilon_F(0)/k_BT \gg 1$) the Stoner criterion derived in [8] is valid, that is $U \approx 2\varepsilon_F(0)$.

Plots of the function $a(y_0,\xi)$ in two extreme cases, $\xi\to 0$ and $\xi\to 1$ [Eqs. (30)-(31)], are illustred in Fig. 2. The band delimited between these two curves represents regions in the plane $(y_0, u/y_0)$ where solutions $\xi\in(0,1]$ exist (except for the trivial one, $\xi = 0$) to cancel the derivative $\partial(\Delta w)/\partial\xi$. These additional solutions lie in the region where, at $T = 0$, the Stoner criterion is not satisfied: $u/y_0 \leqslant 2$.

In Fig. 2, one may identify three regions, as function on the behaviour of the energy $\omega(u, y_0, \xi)$. Region (I), where $\xi = 0$, represents a maximum of ω. Here the paramagnetic state is unstable, and the ferromagnetic state has lower energy. The energy dependence on the asymmetry parameter is a concave parabola (Fig. 2 from [8]). Region (III), where $\xi = 0$, represents a minimum of ω. Here the paramagnetic state is the most stable, and the energy dependence is a convex parabola (Fig. 2 from [8]).

An interesting remark is that, by taking into account the temperature effects, the ferromagnetic region is more extended in the plane $(y_0,\ u/y_0)$. Normally, according to [1], ferromagnetism should occur for $u/y_0 > 2$, whereas here a "tail" representing ferromagnetic states penetrates into the $T = 0$ paramagnetic region. In the extreme case of very large temperatures $y_0\to 0$, the ferromagnetic state might be installed even at $u/y_0\to 1$. This has troubling consequences which will be discussed in a subsequent paragraph, after ellucidating all regions in Fig. 2.

5. Co-existence of stable paramagnetism and ferromagnetism (of which one is stable)

In region II from Fig. 2, the paramagnetic state $\xi = 0$ is still a minimum, but the energy derivative $\partial(\Delta w)/\partial\xi$ has a second extremum $\xi_0\in(0,1]$, which is a maximum, as in Fig. 3. Consequently, in this region one may speak about two stable states, the paramagnetic $\xi = 0$, and the ferromagnetic $\xi = 1$. In fact, by taking into account the observations from Sec. 2, the maximum allowed polarization is not $\xi_{\max} = 1$, but $\xi_{\max} = 1-(\ln 2)y_0^{-1}$, according to Eq. (10).

In the following, we will suppose that no other limitation (e.g. Hund's rules) occurs for ξ to take the maximum allowed value, $\xi_{\max}$, in this region.

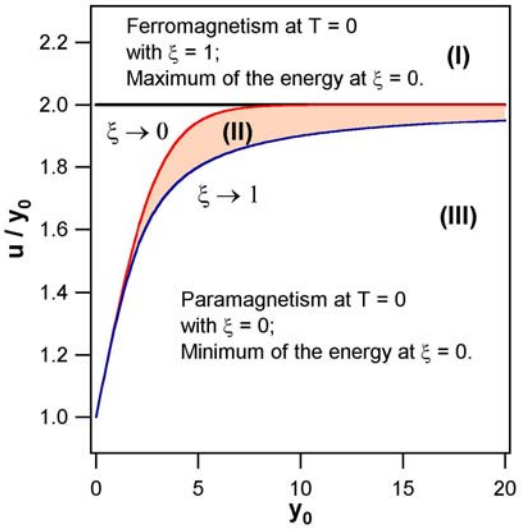

Fig. 2. Regions delimited in the $(y_0, u/y_0)$ plane. In the $T = 0$ case, the upper region with $u/y_0 > 2$, for any y_0, corresponds to ferromagnetism, while the lower region, with $u/y_0 \leqslant 2$ corresponds to paramagnetism. For the discussion of the finite temperature case, see the text for details.

Fig. 3 represents typical energy dependencies in Region II. Fig. 3(a) and Fig. 3(b) represent energy curves by keeping fixed $y_0 = 5$ and 10 respectively, for several values of u. Fig. 3(c) presents similar dependencies, obtained by fixing $u = 20$ and varying y_0.

It may be seen that Region II is rather narrow in the plane (y_0, u). Practically, this two-extremum behaviour is realized roughly in a range of 5-10%

However, an interesting problem to be explored consists in the evaluation of which state (ferromagnetic, or paramagnetic) is the most stable one – the other being metastable. Everything consists then in evaluating the sign of the total energy for $\xi = \xi_{\max}$. By replacing $\xi_{\max}$ from Eq. (10) in the expression of the energy $\omega(u, y_0, \xi)$ – Eq. (22), taking into account that $y_\uparrow(\xi_{\max})$ is given by Eq. (11), and $y_\downarrow(\xi_{\max}) = 0$, one obtains:

$$\begin{aligned}\omega_{\text{ferro}}(u,y_0) &\equiv \omega(u,y_0,\xi_{\max}) \\ &= \frac{1}{2y_0}\left\{\frac{1}{2}\ln^2\left(\frac{e^{2y_0}}{2}-1\right) - \ln^2\left(e^{y_0}-1\right)\right. \\ &\quad + Li_2\left(-\frac{2}{e^{2y_0}-2}\right) - 2Li_2\left(-\frac{1}{e^{y_0}-1}\right) \\ &\quad \left.+\frac{\pi^2}{12}\right\} - \frac{u}{4}\left(1-\frac{\ln 2}{y_0}\right)^2\end{aligned} \tag{32}$$

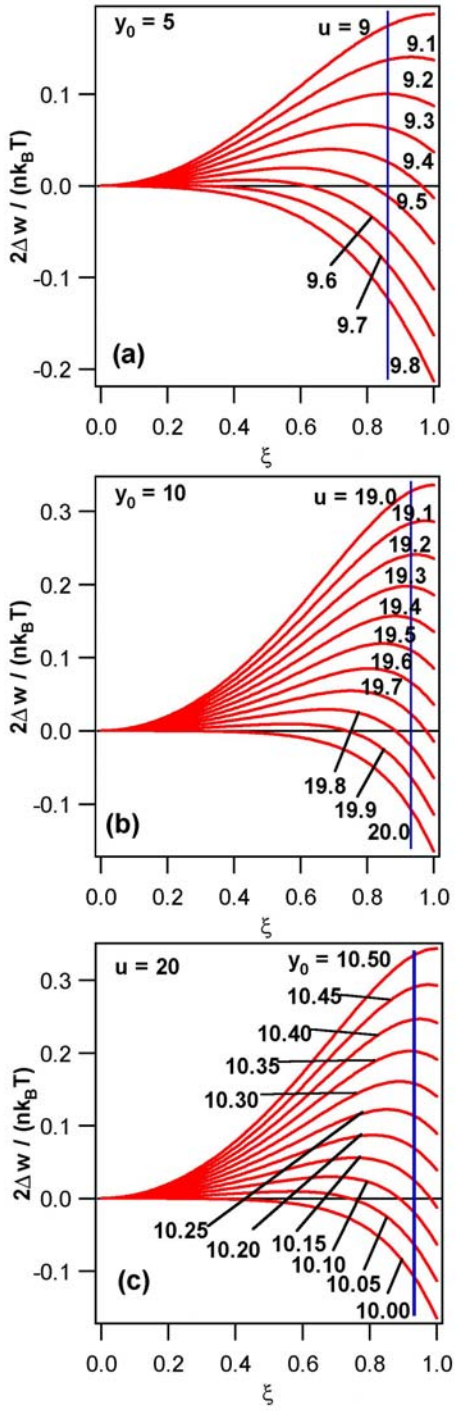

Fig 3. Energy stability curves in region II from Fig. 1. (a) $y_0 = 5$ fixed, u variable; (b) $y_0 = 5$ fixed, u variable; (c) $u = 20$ fixed, y_0 variable. The vertical blue line represents the maximum allowed value for the polarization, according to Eq. (10). In (c), the corresponding values of the maximum polarization lie between two blue lines, corresponding to $y_0 = 5$ and $y_0 = 5$, decrease of the u/y_0 ratio below the $T = 0$ Stoner criterion for the chosen ranges of u and y_0.

A two-dimensional plot of $\omega_{\text{ferro}}(u, y_0)$ is given in Fig. 4.

The paramagnetic region is then defined as the region where $\omega_{\text{ferro}} = \omega_{\text{ferro}}(u, y_0, \xi_{\max}) > 0$. This was evidenced in Fig. 4 by the colored background. More comments on this plot will be made in the next Section.

6. High temperature ferromagnetism. Some key remarks on the possibility of engineering systems with controllable ferromagnetism

Regarding the stability of ferromagnetism with the temperature, the following surprising features appear from the considerations of the last Section. In the following, we will suppose that the 2D system is fully characterized by the values of the Hubbard parameter U and the position of the equilibrium Fermi level $\varepsilon_F(0)$ and we shall investigate the influence of the temperature.

(i) First of all, we remark that the *y* axis of Fig. 2 and Fig. 4 is represented by $u/y_0 = U/\varepsilon_F(0)$ and is therefore independent of the temperature. Consequently, if the $T = 0$, Stoner criterion is satisfied, i.e. $U > 2\varepsilon_F(0)$, the ferromagnetic state is stable for the whole range of y_0. However, there is a limitation in the sense that the first term of Eq. (32) must be finite, i.e. $e^{2y_0} > 2$, then $y_0 > (\ln 2)/2$. When $y_0 \to (\ln 2)/2$, $(1/2)\ln^2\left(e^{2y_0/2} - 1\right) \to \infty$, then the energy becomes infinite for $\xi = \xi_{\max}$ and therefore the ferromagnetism cannot be established with the maximum allowed polarization.

(ii) The most important remark is that there exists a region when $1 < u/y_0 = U/\varepsilon_F(0) < 2$ where the zero temperature Stoner criterion $U/\varepsilon_F(0) > 2$ is *not* satisfied, but ferromagnetism occurs. Moreover, in this region ferromagnetism might occur for *low* values of y_0, i.e. for given $\varepsilon_F(0)$ at *high* temperatures. Let us explore this situation based on Figs. 2 and 4. For low temperatures, i.e. high values of y_0, the system is in the paramagnetic region. By increasing the temperature (i.e. coming with y_0 from infinity towards zero on a straight line of constant u/y_0) at a certain value of y_0, the line given by Eq. (31) is intercepted. In this region, $\xi = 0$ is still a minimum, but the energy curve has a maximum at another value of $\xi \in (0, 1)$. Consequently, towards high values of polarization, the energy of the system decreases, such that the ferromagnetic state with $\xi = \xi_{\max}$ is metastable. By further decrease of y_0, the line corresponding to $\omega_{\text{ferro}} = 0$ is intersected. Here, the energy value at $\xi_{\max}$ becomes negative and consequently the paramagnetic state (although still a minimum, but a local one) becomes the metastable state, whereas the ferromagnetic state is the most stable. For further decrease of y_0, the curve given by Eq. (30) is intercepted and here the paramagnetic state

becomes unstable; then in this region the ferromagnetic state $\xi = \xi_{\max}$ is the only stable state.

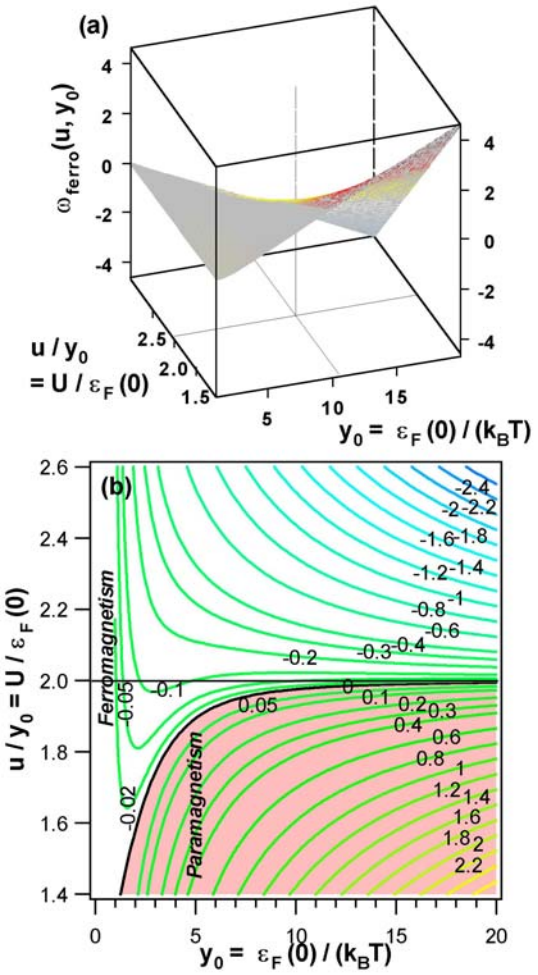

Fig. 4. Plots of the function $\omega_{\text{ferro}}(u, y_0)$: (a) 3D surface plot; (b) contour plot. In (b), the region where $\omega_{\text{ferro}} > 0$, i.e. where the ferromagnetic state at $\xi = \xi_{\max}$ has higher energy than the paramagnetic state ($\xi = 0$), is colored. The ferromagnetic state where $\omega_{\text{ferro}} < 0$ is represented by the white region.

Consequently, in the region investigated here the system is paramagnetic at low temperatures and becomes *ferromagnetic at high temperatures*. This offers the possibility of engineering such systems, i.e. choosing systems where the Hubbard energy and the equilibrium zero temperature Fermi levels are slightly below 2 (e.g. 1.8-1.9).

One may evaluate the temperature where the ferromagnetic state is the most stable. The energy ω changes its sign when $u/y_0 = U/\varepsilon_F(0) > \omega_0(y_0)$, which is the line corresponding to $\omega_{\text{ferro}}(u, y_0) = 0$. From Eq. (32) it follows that:

$$\omega_0(y_0) = \frac{1}{(y_0 - \ln 2)^2}\left[\frac{1}{2}\ln^2\left(\frac{1}{2}e^{2y_0} - 1\right) - \ln^2\left(e^{y_0} - 1\right) + Li_2\left(-\frac{2}{e^{2y_0} - 2}\right) - \frac{\pi^2}{12} - 2Li_2\left(-\frac{1}{e^{y_0} - 1}\right)\right] \quad (33)$$

This dependence is well approximated by:

$$\omega_0 \approx 1.9884 - 1.0872 \cdot e^{-0.48787 y_0} \approx 2 - e^{-y_0/2} \quad (34)$$

From here and from the definition of $y_0 = \varepsilon_F(0)/(k_B T)$, one may compute the temperature where the ferromagnetic state becomes the most stable:

$$k_B T_{\text{ferro}} = \frac{\varepsilon_F(0)}{\ln\left(\dfrac{\varepsilon_F(0)}{2\varepsilon_F(0) - U}\right)} \quad (35)$$

We remind that all the last considerations are valid for $1 < U/\varepsilon_F(0) < 2$.

However, the application of this concept is far from being practical. For ultrathin layers of Fe, and considering that we are allowed to use data for bulk Fe, $\varepsilon_F(0) \approx 6$ eV [11] and $U \approx 8$ eV [12], therefore, according to Eq. (35), one obtains $k_B T_{\text{ferro}} \approx 14.8$ eV, which is more than 170,000 degrees Kelvin! Consequently, the actual "engineering" cannot be applied for systems where the absolute values of U and $\varepsilon_F(0)$ do not exceed some 0.1 eV. This would be the case of semiconductors or diluted magnetic systems, where, indeed, phenomena such as light control of ferromagnetism (by varying $\varepsilon_F(0)$, amongst others) have been recently put into evidence [13].

(iii) As a general rule, most of the energy curves represented in Fig. 3 are "flat" with respect to thermal agitation, i.e. $|\Delta w|/(nk_B T) < 1$. The relative stability between the ferromagnetic and the paramagnetic state is low, as compared to the thermal energy. In this case, simple statistics considerations will give the average value of the polarization as:

$$\langle \xi \rangle = \frac{\int_0^{\xi_{\max}} \xi \exp[-\omega(u, y_0, \xi)] d\xi}{\int_0^{\xi_{\max}} \exp[-\omega(u, y_0, \xi)] d\xi} \quad (36)$$

with $\omega(u, y_0, \xi)$ given by Eq. (22). Plots of $\langle \xi \rangle$ as function on y_0 are represented in Fig. 5. For the clarity of interpretation, plots as function on y_0 and also on $1/y_0 = k_B T/\varepsilon_F(0)$ are presented, the latter presentation [Fig. 5(b)] being easily comparable with experimental temperature dependence on magnetisation $M(T)$. The following remarks are in order:

(a) For large values of $U/\varepsilon_F(0)$, the obtained $M(T)$ curve is almost linear with temperature. A similar behaviour was reported for nickel single layers on Cu(001) [4,16]; however, in Ref. [4] an explanation of this $M(T)$ was given based on two dimensional magnons, whereas in Ref. [16] no explanation of this behaviour was proposed. Here we propose as alternate explanation of the linear decrease of $M(T)$ the 2D band ferromagnetism, concretized by a constant density of states.

We note also that a flat band model (a Friedel density of states [12]) explained well the magnetic properties of Fe/InAs(001) interfaces [12-13]. The effective (orbital and spin) magnetic moments per Fe atom obtained by X-ray magnetic circular dichroism for the above reference at room temperature suggest a value of $\varepsilon_F(0) \approx 0.05$ eV and $U \approx 0.1$ eV.

(b) For smaller values of $U/\varepsilon_F(0) \approx 3-5$, the $M(T)$ decrease has another kind of shape, with a stronger decrease at low temperatures [Fig. 5(b)], followed by an almost linear decrease at higher temperatures. We found exactly this kind of behavior in Ref. [17], regarding 1.9 atomic layers of cobalt deposited on Cu(001) (see Fig. 3(b) from [17]). No explanation of this particular behaviour was given in the above paper. Instead, the data points were qualitatively fitted with a Brillouin ferromagnetic function in order to estimate the Curie temperature. Here we propose that $M(T)$ dependencies such as the one cited above are fully explained by the present model of band two-dimensional ferromagnetism and the present theory allows to estimate the equilibrium Fermi energy as being $k_B \times 280$ K ≈ 0.024 eV, and the Hubbard energy as being $\approx 3\varepsilon_F(0) \approx 0.072$ eV. The above values suggest a strong band narrowing for surface Co films, together with a considerable decrease in the total Hubbard energy (usually it exceeds 8 eV), which partly is due to the decrease in the number of nearest neighbours (4 in a 2D layer, as compared with 12 in the bulk *hcp* structure); and partly to the increase in the interatomic distance induced by the epitaxy process: 2.562 Å for Co/Cu(001), as compared to 2.1 Å nearest-neighbour distance in *hcp* Co.

From the papers dealing with magnetic surfaces cited in the Introduction, a striking similarity with the curves presented in Fig. 5 may be found for the c(2×2) Mn/Cu(001) [6]. Here, the magnetisation vanishes at 55 ± 2 K, which implies $\varepsilon_F(0) \approx 0.0047$ eV and the general shape of the $M(T)$ curve is well fitted by a ratio $U/\varepsilon_F(0) \approx 5$, which gives the Hubbard energy $U \approx 0.024$ eV. The average spacing between two manganese atoms is even lower here, being around 3.6 Å. Consequently, the Hubbard energy strongly decreases with the spacing between adjacent magnetic atoms.

Even more illustrative is the comparison of the magnetisation curve of magnetic vanadium clusters, see Fig. 3 from Ref. [7]. The curve is quite similar to the curve from Fig. 5(b) corresponding to $U/\varepsilon_F(0) = 3$. The relevant parameters which may be obtained for ferromagnetic vanadium are $\varepsilon_F(0) \approx 0.012$ eV and $U \approx 0.036$ eV.

(c) For even smaller values of $U/\varepsilon_F(0) \lesssim 2$, there occurs an unexpected magnetic behaviour with the temperature. Increase of the temperature implies *increase in the magnetisation* of the system. The maximum is attained for a temperature $T_{\max}$, where $k_B T_{\max} \approx \varepsilon_F(0)/(3-5)$, with a slow variation as function on the ratio $U/\varepsilon_F(0)$. Systems with this behaviour have been reported in literature. In [16], this trend is exhibited by some atomic layers of Ni deposited on Cu(001); the same feature seems also visible in some $M(T)$ dependencies reported in [15], concerning interacting trilayers Co/Cu/Ni/Cu(001). More recently and in connexion with our estimate that the present theory should apply especially in diluted magnetic systems are concrete findings of noticeable increase of magnetisation with temperature in cobalt-doped ZnO [18] and partly also in (In,Mn)As [19] diluted magnetic semiconductors.

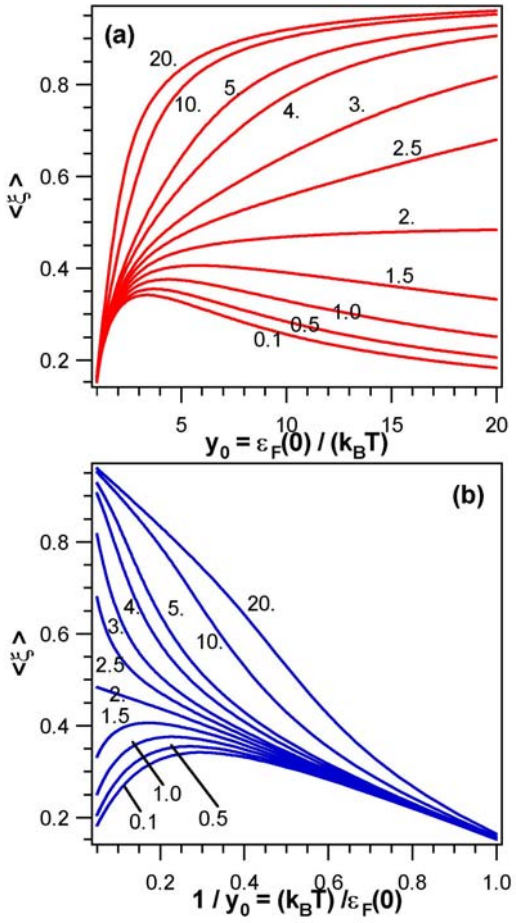

Fig. 5. Statistical average of the polarization degree of the 2D electron gas, as function on y_0 (a) and as function on $1/y_0 = k_B T/\varepsilon_F(0)$ (b), for several values of the ratio $U/\varepsilon_F(0)$, given as numbers associated to each curve; (b) may be easily be converted in a qualitative M(T) dependence.

7. Second order derivative of the energy. The Stoner criterion

The second-order derivative of Δw with respect to magnetic polarization ξ has the expression

$$\frac{1}{nk_BT}\frac{\partial^2(\Delta w)}{\partial\xi^2} \equiv \frac{\partial^2\omega}{\partial\xi^2} = \frac{y_0}{2}\left\{\frac{1-[1+(1+\xi)y_0]e^{-(1+\xi)y_0}}{[1-e^{-(1+\xi)y_0}]^2} + \frac{1-[1+(1-\xi)y_0]e^{-(1-\xi)y_0}}{[1-e^{-(1-\xi)y_0}]^2}\right\} - \frac{u}{2} \quad (37)$$

From this expression it results that

$$\left(\frac{\partial^2\omega}{\partial\xi^2}\right)_{\xi=0} = y_0\frac{1-(1+y_0)e^{-y_0}}{(1-e^{-y_0})^2} \quad (38)$$

The Stoner criterion, which consists in inequality $\left(\frac{\partial^2\omega}{\partial\xi^2}\right)_{\xi=0} < 0$, means that

$$\frac{u}{y_0} > 2\frac{1-(1+y_0)e^{-y_0}}{(1-e^{-y_0})^2} \equiv b(y_0) \quad (39)$$

For the limit of zero temperature, that is

$$\lim_{y_0\to\infty} b(y_0) = 2 \quad (40)$$

the Stoner criterion may be expressed as

$$\varepsilon_F(0) - \frac{U}{2} < 0 \quad (41)$$

and consequently the $T = 0$ Stoner criterion is retrieved.

Towards high temperatures,

$$\lim_{y_0\to 0} b(y_0) = 1 \quad (42)$$

so ferromagnetism is easier obtained at high temperatures, where it suffices that $u/y_0 \approx 1$.

The function $b(y_0)$ defined with the Stoner criterion (Eq. (39)) is represented in Fig. 6, red curve. Above this curve, the system is ferromagnetic, and below it, paramagnetic. This function is compared in Fig. 6 also with the curve defined by $\omega_0(y_0)$ from Eq. (33). We recall here that the meaning of the latter function was the following: above it, the energy corresponding to the maximum polarization is lower than the energy of the paramagnetic state; and below this curve, the paramagnetic state ($\xi = 0$) is the most stable.

As expected, the condition for lower energy in the ferromagnetic state is *more relaxed* than the Stoner criterion. In fact, between both curves from Fig. 6, the paramagnetic state is a minimum (the Stoner criterion is not satisfied, the energy as function on ξ is a convex parabola near $\xi = 0$), but this minimum is local; the energy corresponding to the maximum polarization is lower. The paramagnetic state is *metastable* in this region.

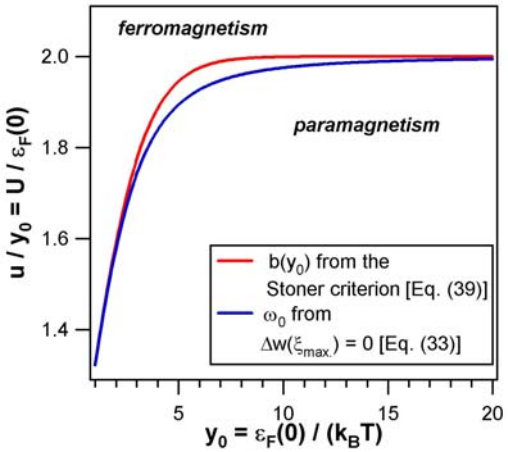

Fig. 6. Comparison between the Stoner criterion of ferromagnetism [eq. (39)] with the conditions that the energy corresponding to the maximum polarization $\xi_{\max}$ is lower than the energy of the paramagnetic state $\xi = 0$ [Eq. (33)].

Thus, Fig. 6 offers the possibility of engineering materials with metastable paramagnetism, which may evolve spontaneusly (by thermal or optical activation) towards the ferromagnetic state. Interesting applications may be foreseen, such as magnetic switches or memories.

8. Conclusions

The temperature-dependent theory of band ferromagnetism is formulated for the simplest case, that of a constant density of states, corresponding to the ideal case of an infinite two-dimensional system. Conditions for ferromagnetism occurence and the Stoner criterion are derived in this temperature-dependent case. Two surprising features are outlined by the model, namely: (i) The existence of a region in the parameters space where ferromagnetism coexists with paramagnetism (both $\xi = 0$ and $\xi = \xi_{\max}$ states are local minima). Obviously, the state with the lower energy is the stable state, and the other is metastable. This offers the possibility of engineering 2D systems, e.g. by surface science methods [2], which may exhibit these features. (ii) The possibility of synthesis of two-dimensional systems where the magnetisation *increases* with the temperature. Some examples from literature compare well with these theoretical findings. (iii) Finally, the present theory is well confirmed by most of the recent experimental findings of surface ferromagnetism from metals which are nonmagnetic in the bulk: Cr [5], Mn [6], and V [7], and also on metal-semiconductor interfaces [12-13] and diluted magnetic semiconductors [13-14].

The Stoner condition, derived in the same way as in Ref. [8], i.e. by analyzing the sign of the second order derivative of the energy as function on ξ in the paramagnetic state ($\xi = 0$), is no longer an immutable condition of the occurence of ferromagnetism. It may happen that this second order derivative at $\xi = 0$ is still positive, implying that paramagnetism results in a local minimum of the energy, but the paramagnetic state is *metastable*. The ferromagnetic state, with maximum polarization, may correspond to a lower energy, see Fig. 3. Therefore, a more relaxed condition for the stability of the ferromagnetic state is derived in the present work, as compared with the Stoner criterion which relies only on the local minimum/maximum character of the energy extremum at zero polarization. This is achieved by putting the condition that the energy of the state with maximum polarization must be lower than the energy of the paramagnetic state, see Eq. (32).

The co-existence of ferromagnetism and paramagnetism is a new feature, together with the possibility of switching relatively easily between the two states. Small variations of the Hubbard parameter U and/or of the equilibrium Fermi energy $\varepsilon_F(0)$ are required to move the paramagnetic state from being the most stable one to being metastable. This opens the possibility of novel devices based on the magnetism of two-dimensional metallic systems. Also, layered materials with anomalous magnetisation *vs.* temperature curves ($\partial M/\partial T > 0$) may be synthesized according to the present theory.

An attractive problem is the phenomenology of the phase transition and the behaviour near the critical point for this system. This is a complex problem; it is still under investigation and will be detailed in a further paper. Nevertheless, we will give a brief outline of this problem. Three alternate methods are currently investigated: (i) The Landau theory of the second order phase transitions, which supposes the development of the energy [Eq. (22)] up to fourth order in the order parameter ξ, then the application of the Landau general equations, derivation of critical exponents, etc. [20]. (ii) A second method to tackle this problem is to compute the entropy of the system, starting with its statistical definition:

$$S = k_{\mathrm{B}} \ln \left(\frac{N!}{N_{\uparrow}! N_{\downarrow}!} \right) \tag{43}$$

In the vicinity of the critical temperature, the energy variation of the system $\delta E \approx T_C \delta S$ is quadratic in ξ, as expected from the general Landau theory [20] and is identified as the contribution of the microscopic exchange term, proportional to $[U + F(y_0)]\xi^2$, where $F(y_0)$ is obtained by series development of the kinetic energy term, Eq. (22). From here, an expression for the critical temperature follows and this implies a limitation of the ferromagnetic region in the diagrams such as presented in Figs. 2, 4, and 5. (iii) An alternate way to treat this problem is to evaluate the fluctuations in the order parameter ξ, i.e. by computing the standard deviation $\Delta\xi = (\langle\xi^2\rangle - \langle\xi\rangle^2)^{1/2}$, by using averages such as Eq. (36). Then, these fluctuations are compared to the average value of the polarization $\langle\xi\rangle$, resulting in a condition for the temperature of the system. The goal of the study outlined briefly above is to obtain perfectly coherent and comparable results from all methods used.

An expected result of all these theories is that there exists a well-defined, finite critical temperature for the 2D band magnetism. This is in contrast with the case of 2D lattice magnetism, where Mermin and Wagner have proven more than four decades ago the absence of ferromagnetic or antiferromagnetic ordering in two-dimensional isotropic Heisenberg systems [21]. An equivalent proof of this theorem was sketched more recently [4], by considering two-dimensional magnons whose action is to suppress ferromagnetism at $T \neq 0$ for infinite 2D systems; it has been shown that the persistence of nonvanishing magnetisation at very low temperatures in 2D systems may be connected to the finite size of the magnetic system investigated. Back to the case of band ferromagnetism, we proved that here nonvanishing magnetisation exists for infinite spatially extended systems, which is an essential difference between the spin and band magnetism in two dimensions. This difference disappears in case of 3D systems.

In conclusion, band ferromagnetism may exhibit surprising features even in the simplest case, that of a constant density of states. It is clear that this work will be continued with the subsequent theory of phase transitions, and also with considerations of band ferromagnetism in systems characterized by other kinds of density of states 1D and 3D systems [$g(\varepsilon) \sim \varepsilon^{-1/2}$, respectively $\sim \varepsilon^{1/2}$], parabolic density of states, linear (and not constant) density of states, and others.

Acknowledgements

This work was *still* financed by the Romanian National Authority for Scientific Research through Contract No. 71-63/2007 MAMAINCOPAE, despite the dramatic reduction of allocated funds to 26.7% of the contracted funds (in 2007) concerning the year 2009.

References

[1] E. C. Stoner, Proc. Roy. Soc. London A **165**, 372 (1938).
[2] S.D. Bader, Surf. Sci. **500**, 172 (2002).
[3] C. A. F. Vaz, J. A. C. Bland, G. Lauhoff, Rep. Progr. Phys. 71, 056501 (2008).
[4] C. M. Teodorescu, Surf. Sci. **601**, 4292 (2007).
[5] M. Albrecht, M. Maret, J. Köhler, B. Gilles, R. Poinsot, J.L. Hazemann, J.M. Tonnerre, C. Teodorescu, and E. Bucher, Phys. Rev. Lett. **85**, 5344 (2000).
[6] Y. Huttel, C. M. Teodorescu, F. Bertran, G. Krill, Phys. Rev. B **64**, 094405 (2001).

[7] Y. Huttel, G. van der Laan, C.M. Teodorescu, P. Bencok, S.S. Dhesi, Phys. Rev. B **67**, 052408 (2003).
[8] C. M. Teodorescu, G.A. Lungu, J. Optoelectron. Adv. Mater. **10**, 3058 (2008).
[9] M. Abramowitz, I. Stegun, Handbook of Mathematical Functions with Formulas, Graphs, and Mathematical Tables, 9th Dover Printing, Dover Publ., New York (1964), p. 1004.
[10] A. D. Polyanin, A. V. Manzhirov, Handbook of Mathematics for Engineers and Scientists, , Taylor & Francis Group, LLC, Boca Raton, FL (2007), p. 1151.
[11] O. Eriksson, L. Nordström, A. Pohl, L. Severin, A. M. Boring, B. Johansson, Phys. Rev. B **41**, 11807 (1990).
[12] C. M. Teodorescu, F. Chevrier, R. Brochier, V. Ilakovac, O. Heckmann, L. Lechevalier, K. Hricovini, Eur. Phys. J. B **28**, 305 (2002).
[13] C. M. Teodorescu, F. Chevrier, R. Brochier, C. Richter, O. Heckmann, V. Ilakovac, P. De Padova, K. Hricovini, Surf. Sci. **482-485**, 1004 (2001).
[14] O. Miura, T. Fujiwara, Phys. Rev. B **77**, 195124 (2008).
[15] A Oiwa, T. Slupinski, and H. Munekata, Appl. Phys. Lett. **78**, 518 (2001); C. Negrila, C. Logofatu, G. Socol, D. Macovei, and C.M. Teodorescu, NSTI Nanotech 2009 Technical Proceedings, in press.
[16] F. May, M. Tischer, D. Arvanitis, J.H. Dunn, H. Henneken, H. Wende, R. Chauvistre, K. Baberschke, J. Physique (France) IV **7** C2-389 (1997).
[17] P. Srivastava, F. Wilhelm, A. Ney, M. Farle, H. Wende, N. Haack, G. Ceballos, K. Baberschke, Phys. Rev. B **58**, 5701 (1998).
[18] H. J. Lee, S. Y. Jeong, C. R. Cho, C. H. Park, Appl. Phys. Lett. **81**, 4020 (2002).
[19] C. M. Teodorescu, M. C. Richter, K. Hricovini, J. Optoelectron. Adv., Mater. **8**, 1200 (2006).
[20] L. D. Landau, E.M. Lifshitz, Statistical Physics, 3rd Edition, Part 1, Landau and Lifshitz Course of Theoretical Physics Vol. 5, Butterworth-Heinemann, Oxford (1980), chapter XIV.
[21] N. D. Mermin, H. Wagner, Phys. Rev. Lett. **17**, 1133 (1966).

*Corresponding author: adrian.lungu@infim.ro